Int. J. Electrochem. Sci., 16 **(2021)** Article ID: 210610, doi: 10.20964/2021.06.10

International Journal of
ELECTROCHEMICAL
SCIENCE
www.electrochemsci.org

Simultaneous Detection of Cd^{2+} and Pb^{2+} with a Bismuth Film/Sulfur and Nitrogen Co-Doped Porous Graphene Electrode

Fengping Liu, Wei Huang[*]*, Zhenfa Zhang, Cuizhong Zhang, Qing Huang, Gang Xiang, Meiyan Liang, Jinyun Peng*[*]

College of Chemical and Food Engineering, Guangxi Normal University for Nationalities, Chongzuo, 532200, China
[*]E-mail: huangwedu641@163.com, pengjinyun@yeah.net

Received: 6 February 2021 / *Accepted:* 13 March 2021 / *Published:* 30 April 2021

In this work, a novel electrochemical sensor based on sulfur and nitrogen co-doped porous graphene (SNPG) is developed for the simultaneous detection of Cd^{2+} and Pb^{2+} by in situ plating bismuth film. The large effective surface area and doped sulfur and nitrogen in porous graphene supply active sites with high affinity toward Cd^{2+} and Pb^{2+} by electrostatic interaction to improve the sensor performance, and the bismuth film improves the stripping voltammetric performance by forming bismuth-metal (Cd, Pb) alloys. Under optimized conditions, this sensor exhibits linearity in the range of 0.05-2 μM for Cd^{2+} and Pb^{2+} with a low detection limit of 0.02 μM for Cd^{2+} and 0.008 μM for Pb^{2+}. Moreover, the proposed sensor was applied for the simultaneous detection of Cd^{2+} and Pb^{2+} in tap water with satisfactory results, suggesting that SNPG is a promising electrode material for detecting heavy metal ions.

Keywords: electrochemical sensor; sulfur and nitrogen co-doped porous graphene; Cd^{2+}; Pb^{2+};

1. INTRODUCTION

Charge transfer and surface electrochemical actives are the two keys to improving the direct determination performance of electrochemical sensors [1]. A porous carbon material with, macro-, meso-, and micropores can greatly improve charge transfer. The macropores can minimize the diffusion distance of ions and electrolytes from each pore, while the meso- and micropores provide large accessible surface areas for ion transport [2]. Recently, porous graphene and its composites have been increasingly studied. Yu et al. reported that lithium-ion batteries based on porous 3D foam structures possessed superior performance, and the porous graphene transport network could improve the electron-

transport efficiency [3]. Huang and his co-workers reported that supercapacitor with porous graphene carbon exhibit an ultra-high energy storage capability of 67 Wh kg^{-1} at an ultrafast discharge time of 45 s [4]. To date, many methods have been used to prepare porous graphene, of which the hydrothermal method combined with freezing-drying is a simple and low-cost approach to obtain graphene materials with high porosity.

On the other hand, heteroatom (e.g., nitrogen, sulfur and boron) doping significantly improves the physical and chemical properties of a matrix, thus increasing the conductivity and the number of electroactive sites [5,6]. Nitrogen doping has been increasingly studied for its higher electronegativity [7]. Zhu et al. reported a supercapacitor based on nitrogen-doped carbon microspheres that fulfilled a high specific capacitance of 228 F g^{-1} at a high current density [8]. Sulfur doping has also attracted more and more attention owing to its lone pair electrons and high electronegativity [9]. Sun and his co-workers developed sulfur-doped carbon spheres as efficient electrocatalysts for the oxygen reduction reaction [10]. Compared with single element doping, nitrogen and sulfur co-doping was more popular owing to its synergistic effect [11]. Aravindaraj and his co-workers reported that dye-sensitized solar cells with nitrogen and sulfur co-doped graphene nanosheet counter electrodes exhibited a high conversion efficiency due to the synergistic effect of co-doping [12]. However, the co-doping of graphene with porous structures has rarely been reported.

Heavy metal ions have drawn global attention due to they pose a threat to life and the environment at very low concentrations, of which Cd^{2+} and Pb^{2+} are two typical major heavy metal pollutants generated from industry, and they have been found in drinking water and aquatic environments. Therefore, methods for the simultaneous determination of Cd^{2+} and Pb^{2+} at the trance level are highly desired. At present, numerous methods are used for Cd^{2+} and Pb^{2+} analysis, such as atomic absorption spectroscopy [13], inductively coupled plasma atomic emission spectrometry [14], and optical methods [15], etc. Although reliable results can be acquired through these methods, sophisticated instrumentation and complicated operation processes are required, which limit their application. Compared with these methods, electrochemical techniques have been considered as powerful analytical methods for detecting heavy metal ions due to their intrinsic advantages of simple instruments, easy operation, high sensitivity, fast response, and low cost [16]. Among these, differential pulse anodic stripping voltammetry (DPASV) has been widely applied for the quantification of trace heavy metals owing to its dramatically high sensitivity. DPASV measurement usually consists of two steps [17]: in the preconcentration step, metal ion in the medium is deposited to the corresponding zero-valent metal onto working electrode surface at a constant potential. In the stripping step, the zero-valent metal is reoxidized to the corresponding cation at a single successive differential pulse potential by applying a voltage sweep. Consequently, a stripping current is produced that is proportional to the metal-ion concentration. The specificity of the method is based on the fact that the oxidation of each metal requires a specific potential. Scheme 1a shows the analysis process of heavy metals by DPASV.

Herein, we develop a simple and facile method for the synthesis of sulfur and nitrogen co-doped porous graphene (SNPG). Graphene oxide (GO) was prepared from graphite using $K_2S_2O_8$ preoxidized followed by the Hummers' method for further oxidation. The sulfur and nitrogen co-doping process was carried out by hydrothermal method with thiourea as a source for both the dopants and reducing agent, followed by freezing-drying at -50 ℃. The obtained sulfur and nitrogen co-doping graphene was porous.

This structure possesses interconnected charge transfer passages, which would be favorable in sensor construction. Scheme 1b shows the procedure for the synthesis of SNPG. Consequently, a new electrochemical sensor for the simultaneous determination of Cd^{2+} and Pb^{2+} was constructed based on this SNPG in the presence of bismuth, SNPG improves the performance of the electrochemical sensor for the analysis of Cd^{2+} and Pb^{2+} because of the synergistic effect of the co-doped sulfur and nitrogen and porous structure. Additionally, bismuth improves the stripping voltammetric performance by the formation of bismuth-metal (Cd, Pb) alloys. The resulting sensor exhibits excellent analytical performance, suggesting that SNPG can be a promising material for electrochemical heavy metal sensors.

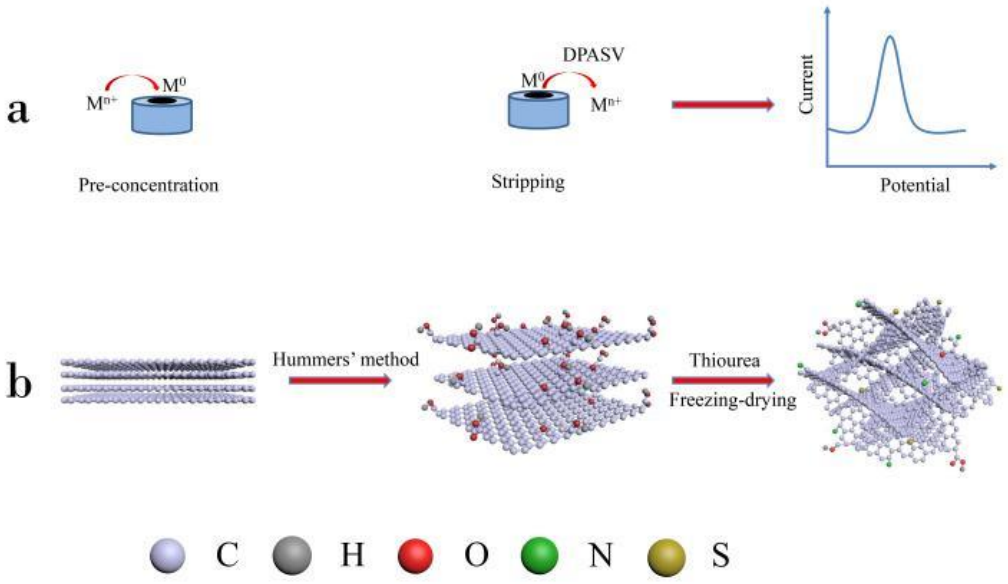

Scheme 1. Analysis process of heavy metals by DPASV (a), the procedure for the synthesis of SNPG.

2. EXPERIMENTAL

2.1 Chemicals and apparatus

Graphite oxide, cadmium nitrate, lead nitrate, bismuth nitrate, sodium acetate, acetic acid and ethanol were obtained from Sinopharm Chemical Reagent (Shanghai, China). Thiourea was acquired from Aladdin (Shanghai, China). Nafion (5 wt. %) was purchased from Sigma-Aldrich (Shanghai, China) and diluted with ethanol to obtain a 0.5 wt. % solution. All chemicals were of analytical grade and used without further purification. Acetate buffer solutions (0.1 M) were prepared by mixing a balanced amount of 0.1 M acetic acid and 0.1 M sodium acetate. All solutions were prepared with deionized water.

The morphology of SNPG was studied by EVO-18 scanning electron microscope (Zeiss, Germany) and transmission electron microscopy (Tecnai 12, Holland). Elemental analysis was

performed on an energy-dispersive X-ray spectroscopy (EDS, Oxford, UK) attached to the scanning electron microscope. Electrochemical experiments were performed on a CHI 660D electrochemical workstation (Shanghai, China) with a conventional three-electrode system consisting of a bare glassy carbon electrode (GCE, Gaossunion, China) or modified electrode as working electrode, a platinum column as the auxiliary electrode and Ag/AgCl (saturated. KCl) as the reference electrode.

2.2 Preparation of sulfur and nitrogen co-doped porous graphene

SNPG was synthesized according to a previous report with slight modification [18]. First, GO was prepared according to an improved Hummer's method [19], after which 90 mg of thiourea was added to 70 mL of a 0.4 mg mL^{-1} GO solution. The solution was sonicated for several minutes and then transferred into a high pressure reactor, which was placed in an oven and maintained at 180 ℃ for 12 h. Then, the autoclave was allowed to cool to room temperature, and the resulting product was washed with distilled water. This was followed by freeze-drying at -50 ℃ overnight in a vacuum. The resulting product was denoted as SNPG.

2.3 Preparation of the modified electrode

The bare GCE (Φ=3 mm) was polished with a 0.05 μm alumina slurry. Then the sample was ultrasonically cleaned with water and ethanol successively before being dried with nitrogen. 5 mg SNPG was dispersed into 5 mL of ethanol to obtain 1 mg/mL SNPG suspensions. Then, 5 μL of the suspensions was dropped on the GCE surface. Finally, 1 μL of 0.5% Nafion was subsequently coated onto the SNPG modified electrode to improve the stability of the modified electrode. The final obtained electrode was denoted as SNPG/GCE. For comparison, GO/GCE was prepared via a similar route.

2.4 Electrochemical detection of Cd^{2+} and Pb^{2+}

DPASV was carried out for the determination of Cd^{2+} and Pb^{2+}. First, the preconcentration of Cd^{2+} and Pb^{2+} on the SNPG/GCE surface was achieved at a deposition potential of -1.1 V for 300 s in 10 mL 0.1 M acetate buffer (pH 4.5) containing 200 μM Bi(III). The stripping process was subsequently performed in the potential range of -1.0 V to -0.5 V for the individual determination of Cd^{2+} and -1.0 V to -0.3 V for the individual determination of Pb^{2+} and simultaneous determination of Cd^{2+} and Pb^{2+}.

3. RESULTS AND DISCUSSION

3.1 Characterization of SNPG

The morphology and microstructure of SNPG were investigated using SEM and TEM (Fig. 1a, band c). The SEM images revealed that the sample has a loose, well-bedded and porous structure, which

was formed due to the flaky graphene curled or interconnected during the freeze-drying process [20]. The interpenetrated hierarchical structure is essential for promoting electron transfer and increasing the number of active sites [21]. In addition, Fig. 1c shows that the transparent sheets of graphene with wrinkled and folded features, in agreement with the SEM results.

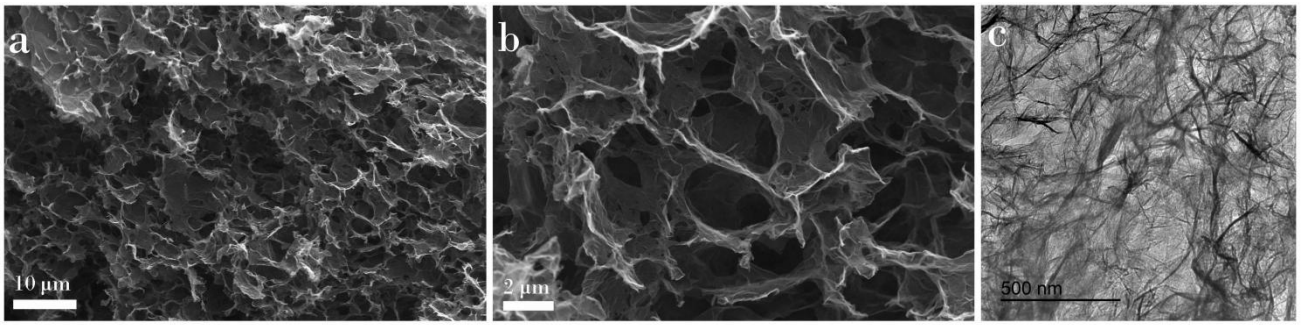

Figure 1. SEM (a,b) and TEM (c) images of SNPG.

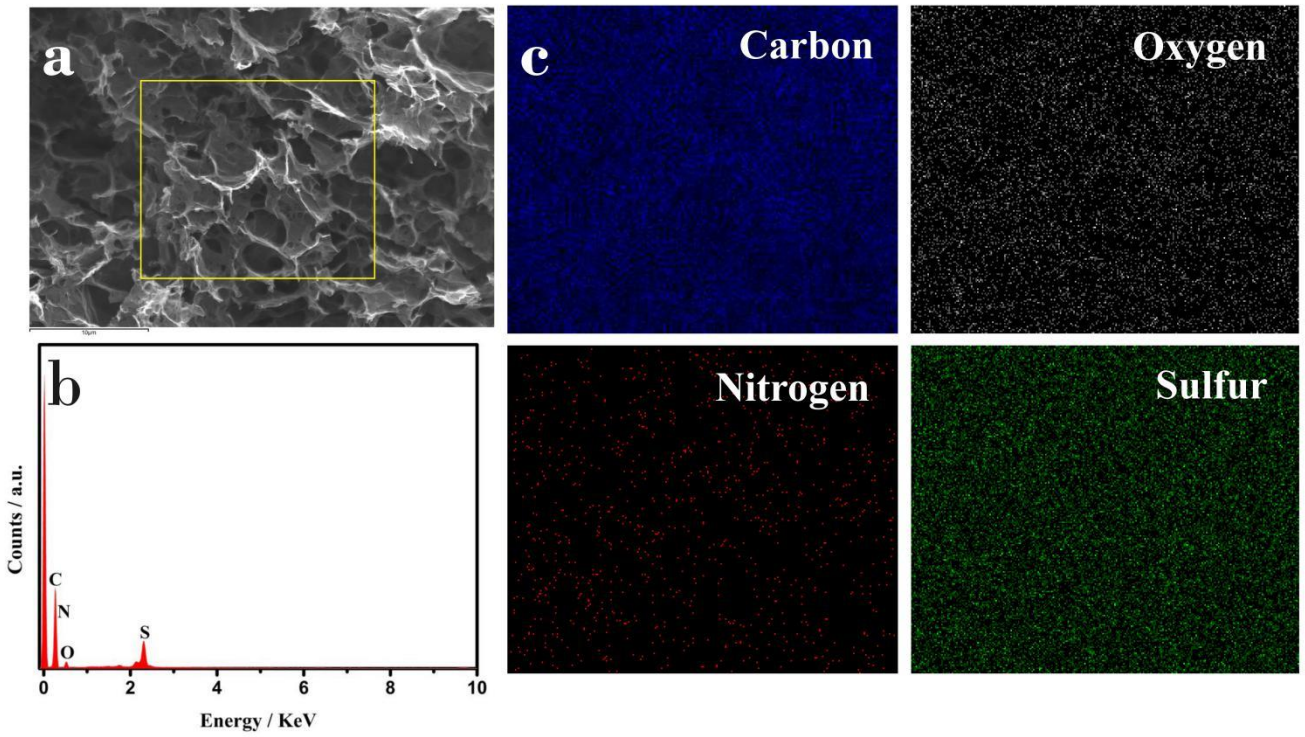

Figure 2. SEM image of SNPG (a), and corresponding EDS spectrum (b) and mapping images of carbon, oxygen, nitrogen and sulfur (c).

To confirm the doping of sulfur and nitrogen in the SNPG sample, EDS was carried out (Fig. 2a-c). The EDS spectroscopy analysis suggests the presence of carbon, oxygen, nitrogen and sulfur, and the EDS mappings show a uniform distribution of carbon, oxygen, nitrogen and sulfur throughout the porous

graphene, indicating the successful doping of nitrogen and sulfur within the porous graphene. Moreover, the quantities of sulfur and nitrogen in SNPG were determined to be 3.33 and 6.09 at.%, respectively. The C/O ratio in SNPG was measured to be 3.61. A low C/O ratio in the SNPG indicates that the oxygen-containing functional groups in GO were weakly reduced during the hydrothermal process, and thiourea can act as the reducing agent as well as a dopant source [12].

3.2 Electrochemical behaviors of different electrodes

Fig. 3a shows the DPASV behavior of 0.5 μM Cd^{2+} and Pb^{2+} at bare GCE, GO/GCE, SNPG/GCE and Bi/SNPG/GCE in 0.1 M acetate buffer solution (pH 4.5) at -1.1 V for 240 s. No stripping peak was observed at GO/GCE due to the poor conductivity of GO, and only a small stripping peak from Pb^{2+} was obtained at the bare GCE. In contrast, two stripping peaks for Cd^{2+} and Pb^{2+} at the SNPG/GCE were observed and the stripping currents were greatly enhanced. This result indicates that the enlarged electroactive surface area and doped sulfur and nitrogen of the SNPG will beneficial for the accumulation of the target analytes due to their high affinity to heavy metal ions. Moreover, the good conductivity and porous structure of the SNPG materials can further facilitate the charge transfer at the electrode. After the addition of 200 μM Bi(III) into the solution, the stripping signals of the Bi/SNPG/GCE were increased by approximately 6.9 times for Cd^{2+} at -0.8 V and 1.1 times for Pb^{2+} at -0.5 V in comparison to SNPG/GCE, which due to the formation of bismuth-metal (Cd, Pb) alloys could dramatically improve the stripping voltammetric performance [22]. The potential difference of 300 mV between the stripping peaks of Cd^{2+} and Pb^{2+} makes it possible to simultaneously determine these two ions.

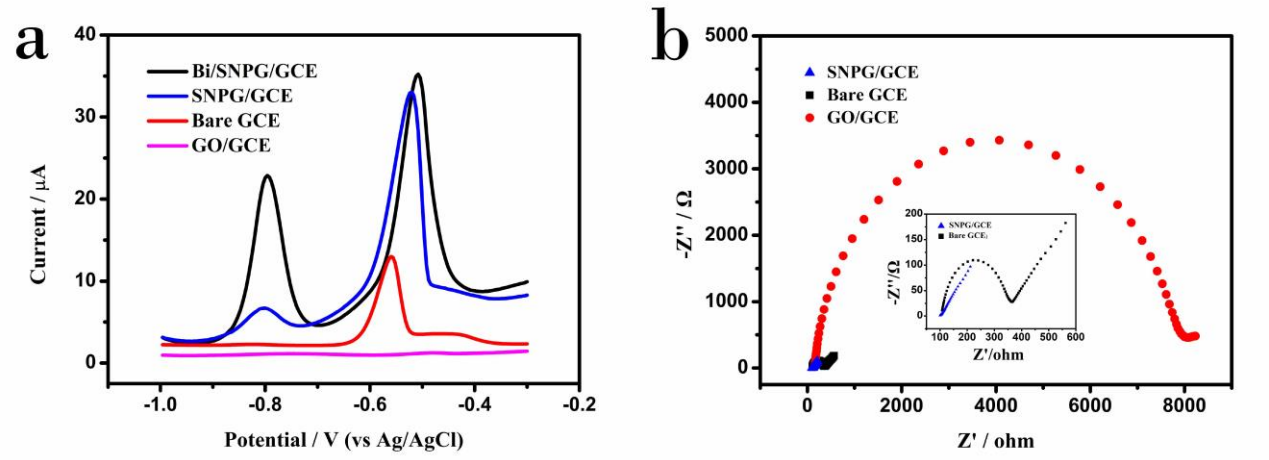

Figure 3. (a) DPASV curves at the bare GCE, GO/GCE, SNPG/GCE and Bi/SNPG/GCE in 0.1 M acetate buffer solution (pH 4.5) containing 0.5 μM Cd^{2+} and Pb^{2+}. (b) EIS curves of the bare GCE, GO/GCE and SNPG/GCE in 5.0 mM $[Fe(CN)_6]^{3-/4-}$ containing 0.5 M KCl.

EIS was applied to study the interfacial properties of the electrodes. As shown in Fig. 3b, the EIS curves consist of a semicircle and a line that represent the electron-transfer resistance (R_{et}) and diffusion limited processing, respectively. The R_{et} of the bare GCE was 295 Ω. After the GCE was modified with

GO, the R_{et} significantly increased, suggesting that a regression of the transfer process at the modified electrode surface. In contrast, the R_{et} of SNPG/GCE decreases sharply compared to that of GO/GCE, implying that the SNPG possesses good conductivity and faster electron transfer, which agrees with the DPASV results.

3.3 Optimization of the determination conditions

To establish the best stripping responses of Bi/SNPG/GCE toward the simultaneous detection of Cd^{2+} and Pb^{2+}, several crucial affecting factors such as the dropping volume, pH, concentration of Bi(III), deposition potential and preconcentration time were examined.

Fig. 4a demonstrates the influence of dropping volume on the stripping responses of the Bi/SNPG/GCE. Slight increased peak currents were observed with the amount of dropping volume increasing in the range of 1-3 μL. This result was due to the enlarged surface area with the increased number of active sites for metal adsorption as well as the enhanced electron transfer rate on the electrode surface. However, when the dropping volume was exceeds 3 μL, the peak currents decreased dramatically due to the thicker modifying membrane impeding the transportation of Cd^{2+} and Pb^{2+} [23]. Consequently, a dropping volume of 3 μL was the optimal value and was selected for the following measurements.

Fig.4b shows the influence of different pH values on the electrochemical responses of Bi/SNPG/GCE. The stripping signals of Cd^{2+} and Pb^{2+} increased with a pH ranging from 3.5 to 4.5. After the pH value is above 4.5, the stripping signals of Cd^{2+} and Pb^{2+} decreased with increasing pH value. The lower pH values lead to a decrease in the stripping signals owing to the protonation of the hydrophilic groups of SNPG. The stripping signals decreased at higher pH values probably due to the hydrolysis of metal ions [22]. Therefore, a pH of 4.5 was chosen in this work.

As shown in Fig. 4c, the effect of the Bi(III) concentration was optimized from 0 to 325 μM. The stripping responses for Cd^{2+} and Pb^{2+} increased from 0 to 200 μM and decreased in the range of 200 to 325 μM, with the maximum value at 200 μM. The decrease in the stripping response after the maximum value may be owing to the fact that the thick bismuth film hinders mass transfer [24]. Thus, Bi(III) concentration of 200 μM for was optimal and chosen for the subsequent experiments.

Fig. 4d exhibits the effect of the deposition potential in the range of -1.4 to -0.9 V. The current responses for Cd^{2+} and Pb^{2+} increased from -1.4 to -1.1 V. At a deposition potential more positive than -1.1 V, the current responses decreased because of the incomplete reduction of the bismuth-metal alloys [24]. Thus, -1.1 V was selected as the optimal deposition potential.

It is known that the preconcentration time for the stripping analysis of heavy metals is crucial. As indicated in Fig. 4e, the stripping peak currents increased greatly for Cd^{2+} and Pb^{2+} with deposition time from 100 to 300 s, suggesting that a longer deposition time would promotes the accumulation of metal ions on the Bi/SNPG/GCE interface. After 300 s, the stripping peak currents decreased sharply, which may be due to the electrode fouling from the accumulation of excess ions on the surface of the electrode at longer deposition time [25]. Thus, a 300 s deposition time was selected for further studies.

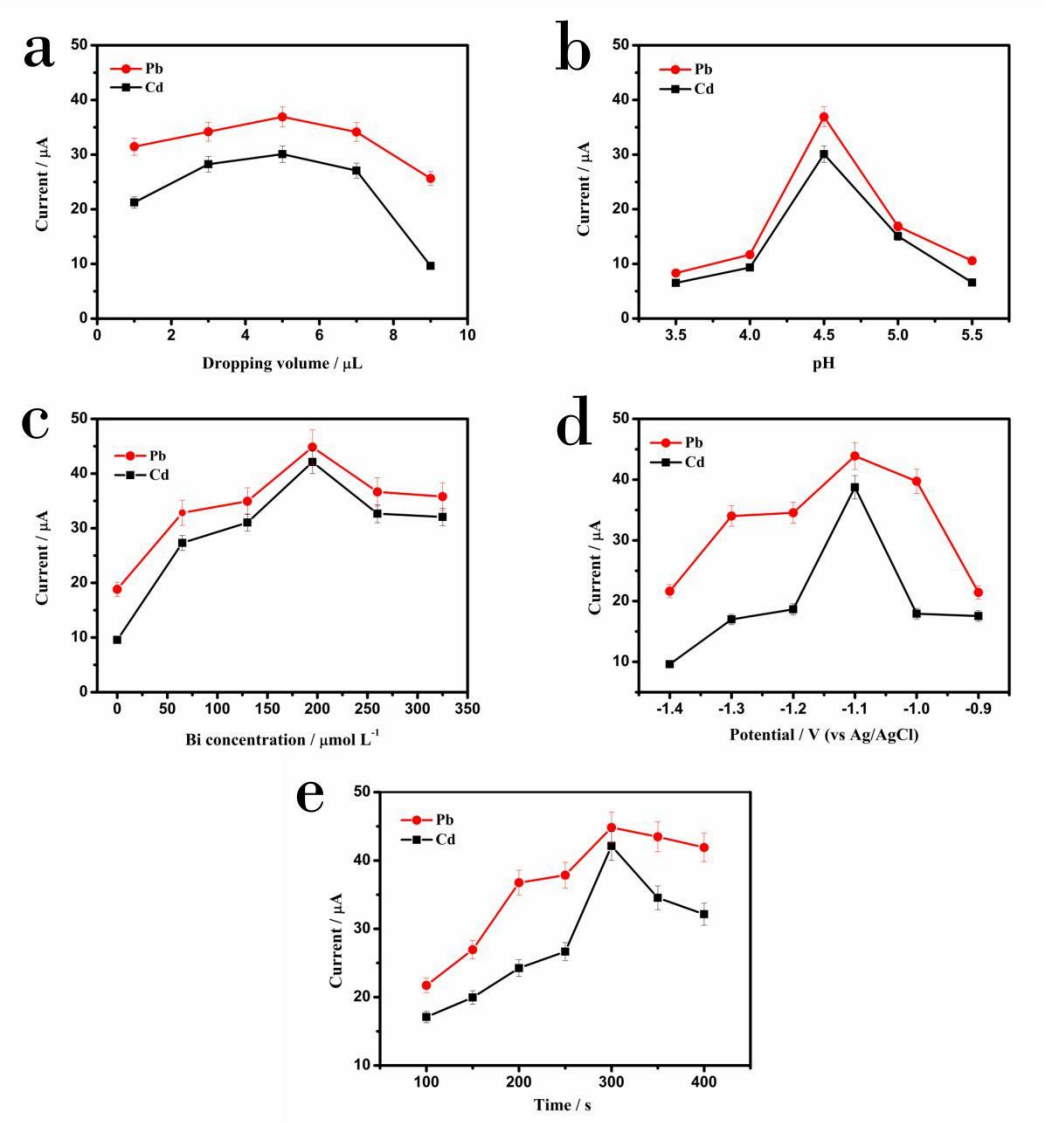

Figure 4. Effect of experimental parameters on the DPASV peak currents of 0.5 μM Cd^{2+} and Pb^{2+} in 0.1 M acetate buffer solution (pH 4.5). (a) dropping volume, (b) pH value, (c) Bi(III) concentration, (d) deposition potential, (e) deposition time.

3.4 Individual/simultaneous determination of Cd^{2+} and Pb^{2+}

The analytical performance of Bi/SNPG/GCE in the individual and simultaneous detection of Cd^{2+} and Pb^{2+} under optimized conditions was evaluated by DPASV. Fig. 5a exhibits the stripping peak currents for different concentrations of Cd^{2+}. The inset of Fig. 5a illustrates that the peak currents were linear with Cd^{2+} concentrations ranging from 0.075 - 2.3 μM. The correlation equation was I_p (μA) = 0.8941 C (μM) - 0.1021 (R^2=0.993). The limit of detection (LOD) calculated to be 0.031 μM based on 3δ/S, where δ represents the standard deviation of the response and S is the slope of the calibration curve. Regarding the individual analysis of Pb^{2+} (Fig. 5b), the stripping peak currents were linear with Pb^{2+} concentrations in the range of 0.04 - 2 μM. The correlation equation was I_p (μA) = 1.3065 C (μM) - 0.0929 (R^2=0.998) with a LOD of 0.007 μM (3δ/S).

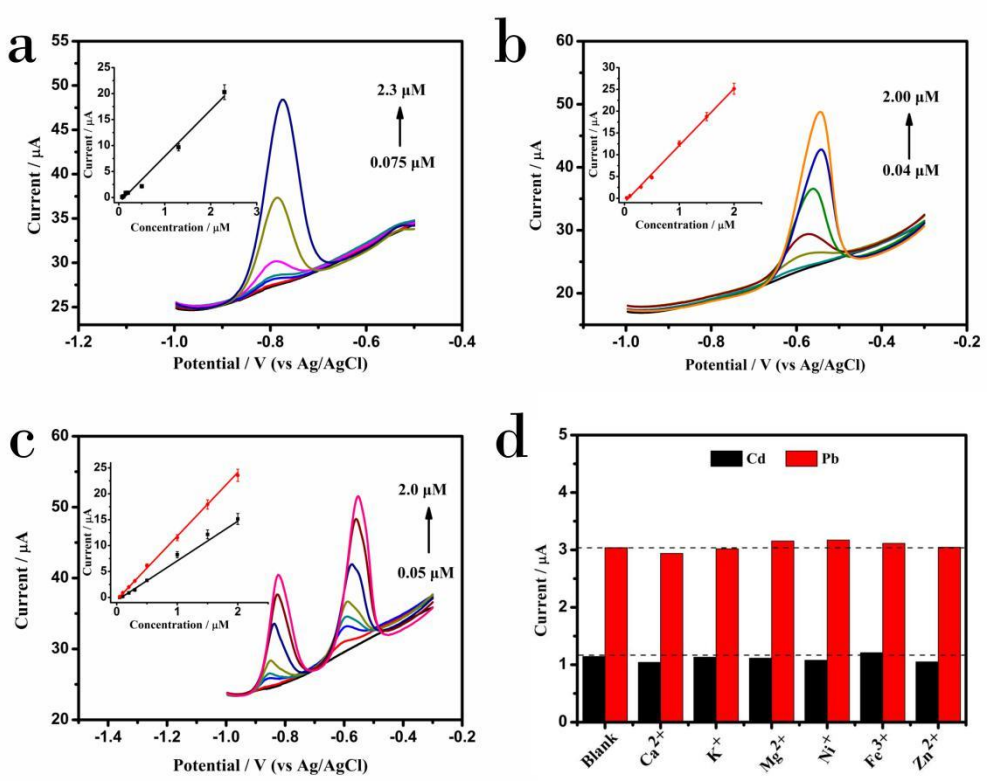

Figure 5. DPASV curves of different concentrations of Cd^{2+} (a), Pb^{2+} (b), Cd^{2+} and Pb^{2+} (c); the insets are the calibration curves of the stripping currents vs the concentration of analytes. (d) Results of the interference study on the response of metal ions (100-fold concentration).

Table 1. Comparison of the proposed sensor for determination of Cd^{2+} and Pb^{2+} with others.

Electrode	Method	Linear range (μM)		Limit of detection (μM)		Ref.
		Cd^{2+}	Pb^{2+}	Cd^{2+}	Pb^{2+}	
Bi/CPE	SWASV	0.09-0.9	0.09-0.9	0.01	0.004	[26]
Bi/CNT/SPE	SWASV	0.02-0.89	0.10-0.48	0.006	0.006	[27]
RGO/Bi/CPE	DPASV	0.18-1.07	0.10-0.58	0.025	0.004	[28]
Nitrogen-doped Microporous Carbon	DPASV	0.018-0.89	0.002-0.48	0.013	0.0002	[29]
Bi/NF/thiolated/GCE	SWASV	0.0008-0.18	0.0004-0.14	0.0003	0.0002	[30]
Bi/Cu/SPE	SWASV	10.06-11.99	1.30-13.00	0.53	0.83	[31]
BiNPs@NPCGSc/GCE	SWASV	0.08-0.8	0.06-0.6	0.004	0.003	[32]
Bi/SNPG/GCE	DPASV	0.05-2	0.05-2	0.02	0.008	This work

Fig. 5c displays the simultaneous determination of Cd^{2+} and Pb^{2+}. The sensor has an excellent linear concentration range of 0.05-2 μM for both Cd^{2+} and Pb^{2+} with linearization equations of I_p (μA) = 1.1316 C (μM) - 0.0065 (R^2=0.994) and I_p (μA) = 0.8175 C (μM) - 0.0601 (R^2=0.995), respectively. The

detection limits were calculated for Cd^{2+} and Pb^{2+} to be 0.023 and 0.008 μM (3δ/S), respectively. We also compared the electrochemical performance of the proposed sensor with that of the previously reported. As shown in Table 1, suggesting that the analytical performance of this sensor is comparable or even better than that of previous reports.

3.5 Evaluation of mutual interferences

In order to evaluate the selectivity of the proposed sensor, 100-fold Ca^{2+}, K^{-}, Mg^{2+}, Ni^{2+}, Fe^{3+}, Zn^{2+} were added to the 0.1 M acetate buffer solution (pH 4.5) containing Cd^{2+} and Pb^{2+}, and these solutions were examined under optimized conditions. As shown in Fig. 5d, there were slight changes in the stripping peak currents of Cd^{2+} and Pb^{2+}, suggesting that the sensor has good selectivity for the determination of Cd^{2+} and Pb^{2+}.

3.6 Reproducibility measurements

The reproducibility of the proposed sensor was evaluated by 10 repetitive measurements of 0.5 μM Cd^{2+} and Pb^{2+} under optimized conditions (Fig. 6a). The stripping peak currents of Cd^{2+} and Pb^{2+} on Bi/SNPG/GCE were reproducible with a relative standard deviation of 1.30% for Cd^{2+} and 1.92% for Pb^{2+}. The current was also tested three times with 5 different electrodes. The RSD was 2.50% for Cd^{2+} and 2.66% for Pb^{2+} (Fig. 6b). These results show that the electrode has a good reproducibility.

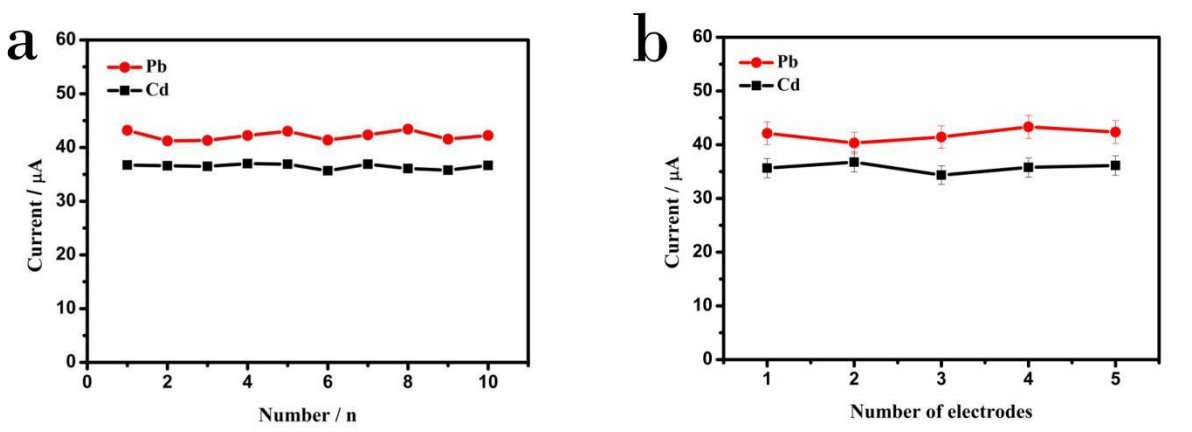

Figure 6. (a) Reproducibility measurements of 0.5 μM Cd^{2+} and Pb^{2+} (10 times), and (b) reproducibility measurements of 0.5 μM Cd^{2+} and Pb^{2+} on 5 different electrodes under optimized working conditions.

3.7Analytical to real environments

To evaluate the accuracy in practical applications, the Bi/SNPG/GCE was used to detect Cd^{2+} and Pb^{2+} in local tap water sample. The measurement results of the sample were shown in Table 2. The

recovery percentages of Cd^{2+} and Pb^{2+} are 92.0-104.0% and 97.0-104.0%, respectively, indicating that the prepared electrode shows high promise for the detection of Cd^{2+} and Pb^{2+} in real samples.

Table 2. Results for the determination of Cd^{2+} and Pb^{2+} in tap water sample

Sample	Added (μM)		Found (μM)		Recovery(%)	
Tap water	Cd^{2+}	Pb^{2+}	Cd^{2+}	Pb^{2+}	Cd^{2+}	Pb^{2+}
	0	0	N.D	N.D	N.D	N.D
	0.5	0.5	0.46	0.52	92.0	104.0
	1.0	1.0	1.03	0.97	103.0	97.0
	1.5	1.5	1.56	1.46	104.0	97.3

N.D: not detected

4. CONCLUSION

In summary, a bismuth-modified SNPG electrode was prepared and applied for the individual and simultaneous determination of Cd^{2+} and Pb^{2+} by using DPASV. The good electrical conductivity and increased number of active sites of SNPG significantly improved the electrochemical responses for the determination of Cd^{2+} and Pb^{2+}. The proposed sensor demonstrated a low limit of detection and good reproducibility toward Cd^{2+} and Pb^{2+} detection. In addition, this sensor was successfully employed for the detection of Cd^{2+} and Pb^{2+} in tap water. The proposed method shows high potential for application in the environmental monitoring of Cd^{2+} and Pb^{2+}.

ACKNOWLEDGEMENTS
The authors gratefully acknowledge the Foundation of the Guangxi Normal University for Nationalities (2018QN037, 2020YB010) and the Guangxi Higher Institutions Scientific Research Project (2019KY0771, 2021KY0770).

References

1. Y. L. Qi, Y. Cao, X. T. Meng, J. Cao, X. W. Li, Q. L. Hao, W. Lei, Q. H. Li, J. Li, and W. M. Si, *Sens. Actuators B. Chem*., 279 (2019) 170.
2. Y. Y. Li, Z. S. Li, and P.K. Shen, *Adv. Mater*., 2 (2013) 2474.
3. H. Yu, D. Ye, T. Butburee, L. Wang, and M. Dargusch, *ACS Appl. Mater. Inter*., 8 (2016) 2505.
4. J. L. Huang, J. Y. Wang, C.W. Wang, and H. N. Zhang, *Chem. Mater*., 27 (2015) 2107.
5. S. A. Wohlgemuth, F. Vilela, M. M. Titirici, and M. Antonietti, *Green Chem*., 14 (2012) 741.
6. Y. Q. Zhang, M. M. Jia, H. Y. Gao, J. G. Yu, L. L. Wang, Y. S. Zou, F. M. Qin, and Y. N. Zhao, *Electrochim. Acta*, 184 (2015) 32.
7. J. R. Zhang, X. Wang, G. C. Qi, B. H. Li, Z. H. Song, H. B. Jiang, X. H. Zhang, and J. L. Qiao, *Carbon*, 96 (2016) 864.

8. D. Z, Zhu, Y. W. Wang, L. H. Gan, M. X. Liu, K. Cheng, Y. H. Zhao, X. X. Deng, and D. M. Sun, *Electrochim. Acta*, 158 (2015) 166.
9. Y. Bide, M. R. Nabid, and F. Dastar, *RSC Adv*., 5 (2015) 6342.
10. Y. Sun, J. Wu, J. H. Tian, C. Jin, and R. Z. Yang, *Electrochim. Acta*, 178 (2015) 806.
11. C. Domínguez, F. J. Pérez-Alonso, S. A. Al-Thabaiti, S. N. Basahel, A. Y. Obaid, A. O. Alyoubi, J. L. Gómez de la Fuente, and S. Rojas, *Electrochim. Acta*, 157 (2015) 158.
12. A. G. Kannan, J. X. Zhao, S. G. Jo, Y. S. Kang, and D. W. Kim, *J. Mater. Chem. A*, 2 (2014) 12232.
13. M. Schneider, É. R. Pereira, D. P. C.de Quadros, B. Welz, E. Carasek, J. B.de Andrade, J. C. Menoyo, and J. Feldmann, *Microchem. J*., 133 (2017) 175.
14. T. Y. Ho, C. T. Chien, B. N. Wang, and A. Siriraks, *Talanta*, 82 (2010) 1478.
15. Y. L. Wang, S. Y. Lao, W. J. Ding, Z. D. Zhang, S. and Y. Liu, *Sens. Actuators B. Chem*., 284 (2019) 186.
16. F. Gao, C. Gao, S. Y. He, Q. X. Wang, and A. Q. Wu, *Biosens. Bioelectron*., 81 (2016) 15.
17. A. Waheed, M. Mansha, and N. Ullah, *Trac-trend. Anal. Chem*., 105 (2018) 37.
18. A. G. Kannan, A. Samuthirapandian, and D. W. Kim, *J. Power Sources*, 73 (2016) 26.
19. J. Chen, B. Yao, C. Li, G. and Q. Shi, *Carbon*, 64 (2013) 225.
20. F. P. Liu, Q. Xu, W. Huang, Z. F. Zhang, G. Xiang, C. Z. Zhang, C. Y. Liang, H. Lian, and J. Y. Peng, *Electrochim. Acta*, 295 (2019) 615.
21. S. Jiang, Y. J. Sun, H. C. Dai, J. T. Hu, P. J. Ni, Y. L. Wang, and Z. Li, *Electrochim. Acta*, 174 (2015) 826.
22. S. Lee, J. Oh, D. Kim, and Y. Z. Piao, *Talanta*, 160 (2016) 528.
23. H. Xu, L. P. Zeng, S. J. Xing, Y. Z. Xian, G. Shi, and L. T. Jin, *Electroanalysis*, 20 (2008) 2655.
24. J. Li, S. J. Guo, Y. M. Zhai, and E. K. Wang, *Anal. Chim. Acta*, 649 (2009) 196.
25. N. Promphet, P. Rattanarat, O. Chailapakul, R. Rangkupan, and N. Rodthongkum, *Sens. Actuators B. Chem*., 207 (2015) 526.
26. S. B. Hočevar, I. Švancara, K. Vytřas, and B. Ogorevc, *Electrochim. Acta*, 51 (2005) 706.
27. G. H. Hwang, W. K. Han, J. S. Park, and S. G. Kang, *Talanta*, 76 (2008) 301.
28. P. K. Sahoo, B. Panigrahy, S. Sahoo, A. K. Satpati, D. Li. and D. Bahadur, *Biosens. Bioelectron*. 43 (2013) 293.
29. L. L. Xiao, H. B. Xu, S. H. Zhou, T. Song, H. H. Wang, S. Z. Li, W. Gan, and Q. H. Yuan, *Electrochim. Acta*, 143 (2014) 143.
30. L. Chen, Z. H. Su, X. H. He, Y. Liu, C. Qin, Y. P. Zhou, Z. Li, L. H. Wang, Q. J. Xie, and S. Z. Yao, *Electrochem. Commun.,* 15 (2012) 34.
31. L. C. S. Figueiredo-Filho, B. C. Janegitz, O. Fatibelilo-Filho, L. H. Marcolino-Juniorb, and C. E. Banks, *Anal. Methods*, 5 (2013) 202.
32. L. Cui, , J. Wu, and H. X. Ju, *Chem. Eur. J*., 21 (2015) 11525.